

# Performance-Driven QUBO for Recommender Systems on Quantum Annealers

Jiayang Niu

s4068570@student.rmit.edu.au

School of Computing Technologies,  
RMIT University

Mark Sanderson

mark.sanderson@rmit.edu.au

School of Computing Technologies,  
RMIT University

Jie Li

hey.jielij@gmail.com

School of Computing Technologies,  
RMIT University

Nicola Ferro

nicola.ferro@unipd.it

Department of Information  
Engineering, University of Padua

Ke Deng

ke.deng@rmit.edu.au

School of Computing Technologies,  
RMIT University

Yongli Ren

yongli.ren@rmit.edu.au

School of Computing Technologies,  
RMIT University

## Abstract

We propose Counterfactual Analysis Quadratic Unconstrained Binary Optimization (CAQUBO) to solve QUBO problems for feature selection in recommender systems. CAQUBO leverages counterfactual analysis to measure the impact of individual features and feature combinations on model performance and employs the measurements to construct the coefficient matrix for a quantum annealer to select the optimal feature combinations for recommender systems, thereby improving their final recommendation performance. By establishing explicit connections between features and the recommendation performance, the proposed approach demonstrates superior performance compared to the state-of-the-art quantum annealing methods. Extensive experiments indicate that integrating quantum computing with counterfactual analysis holds great promise for addressing these challenges.

## Keywords

Quantum Computers, Recommender Systems, Feature Selection

## ACM Reference Format:

Jiayang Niu, Jie Li, Ke Deng, Mark Sanderson, Nicola Ferro, and Yongli Ren. 2018. Performance-Driven QUBO for Recommender Systems on Quantum Annealers. In *Proceedings of Make sure to enter the correct conference title from your rights confirmation email (Conference acronym 'XX')*. ACM, New York, NY, USA, 11 pages. <https://doi.org/XXXXXX.XXXXXXX>

## 1 INTRODUCTION

Compared to traditional transistor-based computers, quantum computers [11, 35, 58], are still in the experimental stage, but demonstrate a higher chance of escaping the local minima when facing optimisation problems [3, 4, 34, 64]. Specifically, Tadashi and Hidetoshi had investigated the theoretical support for the potential performance advantage of quantum annealing in optimisation tasks. Recent research shows that quantum annealing leverages quantum

Permission to make digital or hard copies of all or part of this work for personal or classroom use is granted without fee provided that copies are not made or distributed for profit or commercial advantage and that copies bear this notice and the full citation on the first page. Copyrights for components of this work owned by others than the author(s) must be honored. Abstracting with credit is permitted. To copy otherwise, or republish, to post on servers or to redistribute to lists, requires prior specific permission and/or a fee. Request permissions from permissions@acm.org.

Conference acronym 'XX, June 03–05, 2018, Woodstock, NY

© 2018 Copyright held by the owner/author(s). Publication rights licensed to ACM.

ACM ISBN 978-1-4503-XXXX-X/18/06

<https://doi.org/XXXXXX.XXXXXXX>

tunneling to escape local optima and efficiently explore vast solution spaces, offering a novel approach to tackling large-scale, high-dimensional combinatorial problems [3, 4, 34, 64]. Moreover, Quantum Annealing (QA) naturally aligns with Quadratic Unconstrained Binary Optimization (QUBO) problems [25], enabling us to leverage existing quantum annealers to explore combinatorial optimization problems that are challenging for classical computers to solve [45]. On the other hand, although embedding techniques [26, 28, 29] have effectively alleviated the feature selection problem in recommender systems to some extent, recent studies [20, 27, 33, 36, 62, 66] have emphasized the necessity of further exploring this issue due to challenges related to the storage of large-scale embedding tables and the retrieval efficiency of recommender systems. Moreover, research [17] has shown that reasonably retaining 20%-40% of embedding dimensions in retrieval systems can significantly enhance performance. The QUBO problem, which can be solved quickly and accurately using quantum annealers, has been demonstrated in previous studies [18, 43] to be highly suitable for feature selection problems, as it considers pairwise coupling relationships between features and identifies optimal feature combinations. Furthermore, due to the powerful advantages of quantum annealers in solving combinatorial problems, QUBO is regarded as one of the promising approaches to exploring feature selection problems [42]. However, there are significant challenges when using quantum annealing to solve complicated real world feature selection for recommendation purposes, and this paper investigates this by answering the following questions: **Q1**) While having the potential, how does the instability of a quantum annealer affect the performance of recommender systems? **Q2**) How effective is a quantum annealer in feature selection for recommender systems? **Q3**) Can this emerging quantum platform achieve or even surpass the performance of mature feature selection methods on traditional computers?

In this paper, following existing research, we investigate these questions in the context of QUBO-based feature selection for recommender systems on quantum annealers. Specifically, the QUBO formulation tailored to the feature selection problem in recommender systems is far from straightforward, and the key challenge lies in how to model the relationship between features and the optimization of recommendation problem [25]. One approach is the construction of a Coefficient Matrix  $Q$  (definition provided in Section 3.2), which determines the alignment of the optimization direction of the QUBO problem with the optimization needs of

feature selection. Existing research explored the construction of this coefficient matrix with the similarities between collaborative filtering and content-based models [43], mutual information, correlation, or the similarity between the classification predictions [18]. However, although these existing works used either the ground truth (e.g. classification labels) or the model outcome (e.g. classification predictions), none of them consider the performance of the models (e.g. accuracy in classification or recommender systems).

So, to answer the above research questions, we propose a **PDQUBO** (Performance-Driven Quadratic Unconstrained Binary Optimization). The optimizer constructs the Coefficient Matrix by modeling the relationship between features via counterfactual analysis, which evaluates the changes in the final recommendation performance when excluding each feature and each pair of features, known as counterfactual instances. With counterfactual analysis, PDQUBO has two desirable properties. First, PDQUBO explicitly connects optimizing feature selection with the final recommendation performance rather than being based on either the ground truth or the model outcome only. This makes feature selection performance-driven, which contributes to its effectiveness in terms of generating good recommendations. Second, when modeling the importance of features in PDQUBO, the counterfactual analysis ensures the measure is their relative importance to all other features on recommendation performance, which can contribute to the performance in feature selection itself. Due to these properties, PDQUBO drives the optimization direction of the QUBO problem towards the optimization of recommendation performance. Note, with counterfactual analysis, PDQUBO is independent of what the recommender systems are used (known as *base models*) and what recommendation metrics are employed to measure performance. Finally, given PDQUBO is performance-driven, it provides a unique chance to study the instability of quantum anneals and its performance.

The contributions of this paper are as follows: **i)** The PDQUBO model, which aligns optimization direction to the recommendation performance and considers the hidden relationship among features to allow better optimization. **ii)** Comprehensive analysis of the instability of Quantum Annealers in feature selection for recommender systems, from the perspective of the number of features, the sample size in quantum annealing process, and the difficulties of the feature selection problems. **iii)** Extensive experiments on real-world data, using three different categories of base models, demonstrate that the proposed PDQUBO method outperforms other state-of-the-art quantum annealer-based feature selection algorithms in terms of recommendation accuracy.

## 2 RELATED WORK

### 2.1 Quantum Annealing

**2.1.1 Recent applications:** With the rapid advancement of quantum computing architectures [38, 48], researchers have started to explore the potential of leveraging quantum computers' computational advantages to address certain general problems, particularly in domains frequently confronted with NP-hard optimization challenges [6, 7, 69] and the increasing computational demands of deep learning [2, 8, 12, 14]. Quantum annealers [58], a type of quantum computer, are particularly suited for solving combinatorial optimization problems [11] and QUBO (Quadratic Unconstrained

Binary Optimization) problems. Recent studies have focused on formalizing problems in these areas as QUBO problems to leverage quantum annealers for their solutions. Date et al. [14] attempted to formalize simple machine learning methods as QUBO problems with quantum annealers. Some studies [18, 42, 43] have also focused on utilizing quantum annealers to solve feature selection problems for common tasks in recommender systems and information retrieval. Additionally, recent studies have explored the use of quantum annealers for instance selection in fine-tuning large models, aiming to optimize training time [13, 44].

**2.1.2 Coefficient matrix:** The focus of existing research on quantum annealing based recommender systems is on formalizing problems into QUBO solutions, with the key challenge being how to construct a coefficient matrix  $Q$ . In the context of the cold-start problem in recommender systems, CQFS [43] first trains a recommendation model based solely on user-item interactions, followed by another model trained using features. The coefficient matrix  $Q$  is constructed by comparing the consistency of item similarity between the two models. Although Nembrini et al. [18] mainly evaluates the applicability of quantum annealers in ranking and classification tasks, they also proposed MIQUBO, CoQUBO and QUBO-boosting. Specifically, MIQUBO fills the coefficient matrix  $Q$  with mutual information and conditional mutual information between features and the classification labels, directing the optimization towards using the fewest features to maximize the dependence of the feature set on the classification task. On the other hand, CoQUBO fills the coefficient matrix with the correlation between features and the classification labels, aiming to maximize the relationship between the selected feature set and the classification task. For QUBO-boosting, it constructs the coefficient matrix  $Q$  based on the impact of features on the final classification outcome. Similar to feature selection problems, instance selection using quantum annealers [44] involves embedding the relevance of training documents into the coefficient matrix, thereby identifying a smaller, more relevant training sample set for the task.

### 2.2 Counterfactual Analysis

Deep learning models are often regarded as black-box systems due to their limited interpretability [57, 65]. Counterfactual analysis, as a causal inference tool, enables interpretability by perturbing model inputs or internal structures and observing the resulting changes [23, 54]. This process helps uncover the influence of specific features on model behavior, guiding the design of more concise, robust, and effective models [10, 22, 68]. In the context of recommender systems, counterfactual reasoning has been widely adopted. ACCENT [56] introduced one of the first frameworks to apply counterfactuals to neural recommendation models. CountER [52] explored the impact of perturbing item and user preference scores, revealing key contributors to recommendations. CauseRec [67] improved user representations by replacing concept sequences with counterfactual samples. Other works, such as PSF-RS [70] and CASR [63], have applied counterfactuals to enhance fairness and address data sparsity through feature decomposition and augmentation. Collectively, these methods demonstrate the effectiveness of counterfactual analysis in improving interpretability and performance across various model architectures.

### 2.3 Gaps

The existing feature selection methods using quantum annealers focus on the coefficient matrix of the QUBO problem, attempting to align the optimization direction of the problem with the optimization needs of feature selection. However, existing methods do not align with the performance of the recommendation problem directly. It is hard to keep consistency with the feature selection requirements in recommender systems. For example, information-theory-based [19, 46, 55] feature selection methods like MIQUBO and CoQUBO [18] only incorporate dependencies between features and the classification labels into the coefficient matrix  $Q$ , making it less effective to optimize the model performance directly. Similarly, QUBO-Boosting [18] only uses the model outcomes. Although CQFS [43] incorporates collaborative information, it targets at cold start problem and relies on comparing item similarities from collaborative filtering models and content-based models. On the other hand, in recommender systems, existing work on counterfactual analysis mainly focuses on interpretability, with little attention paid to feature selection. To fill the research gap, we propose PDQUBO, which leverages counterfactual analysis to construct the coefficient matrix by connecting the relationship between features directly to the performance of recommender systems, thereby aligning the optimization direction of the QUBO problem to improve recommendation performance.

## 3 PRELIMINARIES

Assume that we have a dataset  $\mathcal{D} = (\mathcal{U}, \mathcal{V}, \mathcal{F})$  that can be used to train the recommender system, where  $\mathcal{U} = \{u_1, u_2, \dots, u_m\}$ ,  $\mathcal{V} = \{v_1, v_2, \dots, v_n\}$ , and  $\mathcal{F} = \{f_1, f_2, \dots, f_{|\mathcal{F}|}\}$  represent users, items, and features of the items, respectively. Each item  $v_i$  corresponds to a  $d$ -dimensional feature vector, denoted as  $\mathbf{f}_i \in \mathbb{R}^d$ . We use a binary matrix  $B \in \{0, 1\}^{m \times n}$  to represent the user-item interaction matrix, where  $B_{ij} = 1$  indicates that user  $u_i$  has interacted with item  $v_j$ , otherwise  $B_{ij} = 0$ . The base model, i.e. the model for recommendation, is defined as  $G_\Theta$ , where  $\Theta$  represents the model parameters trained on the data  $\mathcal{D}$  and the interaction matrix  $B$ . We can obtain the top- $N$  recommendation list  $\mathcal{R}(u_i, N)$  for a specific user  $u_i$  based on the model  $G_\Theta$ . The top- $N$  recommendations for all users can be written as  $\mathcal{R}(\mathcal{U}, N) = G(\mathcal{D}, B|\Theta)$ .

### 3.1 QUBO

Quadratic Unconstrained Binary Optimization (QUBO) is a common form of optimization problem widely used in quantum computing (such as Quantum Annealers) [25], combinatorial optimization (such as max-cut, graph coloring problems), and machine learning [14] (such as feature selection). It can be specifically formalized as an  $n$ -variable quadratic problem, with the objective of finding a set of solutions that minimize the value of the function, which can be expressed as follows:

$$\min_{\mathbf{x}} Y = \mathbf{x}^T Q \mathbf{x} + \left( \sum_{i=1}^{|\mathcal{F}|} x_i - k \right)^2, \quad (1)$$

where  $Y$  corresponds to the ground state energy in Quantum Annealing (QA) [41, 58], and  $\mathbf{x}$  is a binary vector of length  $|\mathcal{F}|$ , which denotes the size of the feature section  $\mathcal{F}$ , with each element  $x_i$  of

the vector being either 0 or 1. *Coefficient matrix*  $Q$  is a symmetric matrix, where each element represents the relationship between the elements of  $\mathbf{x}$ .  $|\mathcal{F}|$  is the total number of features. In the context of feature selection,  $x_i \in \mathbf{x}$  is related to whether their corresponding features are selected; the elements in  $Q$  represents the relationship between features and the optimization problem to solve, determining the optimization direction of the QUBO problem. To control the number of selected features, a penalty term  $\left( \sum_{i=1}^{|\mathcal{F}|} x_i - k \right)^2$  have been added [18], where  $k$  denotes the number of selected features.

### 3.2 Coefficient Matrix $Q$

The values of the coefficient matrix  $Q$  represent the relationship between features and the optimization problem to solve. For the feature selection problem in recommender systems, let  $\text{Indiv}(f_i)$  represent the contribution of feature  $f_i$  to the performance of the recommendation model, while  $\text{Comb}(f_i, f_j)$  indicate the contribution to recommendation performance when both features  $f_i$  and  $f_j$  are selected together. The optimization goal is to maximize the contribution of the selected feature set to the model's performance. So,  $Q$  can be formulated as:

$$Q_{ij} = \begin{cases} -\text{Comb}(f_i, f_j) & \text{if } i \neq j \\ -\text{Indiv}(f_i) & \text{if } i = j. \end{cases} \quad (2)$$

## 4 Performance Driven QUBO

We present the PDQUBO model (the overview as shown in Figure 1) to solve QUBO problems for feature selection in recommender systems. Then, we detail how *counterfactual instances* are defined, and how they are used to construct the coefficient matrix  $Q$ .

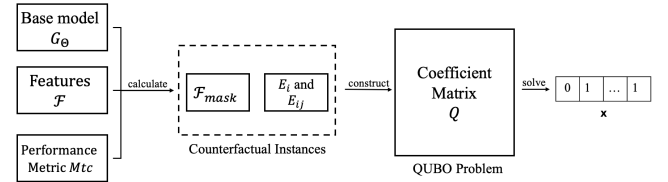


Figure 1: The Overview of PDQUBO

### 4.1 Counterfactual Instances

Counterfactual Analysis adds perturbations to the base model's input variables and observes the changes before and after the perturbations [37, 52, 59, 67]. In this paper, we refer to these changes as **counterfactual instances**. Specifically, similar to [52, 67], in the context of feature selection for recommender systems, we measure the impact of item features by excluding the corresponding feature and analyzing the difference in recommendation performance between the recommendation lists generated by the base model with and without the corresponding feature. Following [9, 51, 60], we define these perturbations in the form of a mask:

$$\mathcal{F}_{\text{mask}} = \mathcal{F} \odot M_c, \quad (3)$$

where  $M_c$  sets certain features of all items to zero. Note, as defined in Equation 1, QUBO solves which features to be selected, so  $\mathcal{F}_{\text{mask}}$  is defined at feature level accordingly. Namely, these excluded features of all items will be the same.

Next, we employ the recommendation performance metric  $Mtc$  (e.g. nDCG [32], or Recall [30]) for Counterfactual Analysis, which is defined as:

$$\begin{cases} E_i = G(\mathcal{F}|\Theta)_{Mtc} - G(\mathcal{F}_{\text{mask}}^i|\Theta)_{Mtc} \\ E_{ij} = G(\mathcal{F}|\Theta)_{Mtc} - G(\mathcal{F}_{\text{mask}}^{ij}|\Theta)_{Mtc}, \end{cases} \quad (4)$$

where  $E_i$  represents the counterfactual instance of removing  $f_i$ , and  $E_{ij}$  represents the counterfactual instance of removing both  $f_i$  and  $f_j$ .  $G(\mathcal{F}|\Theta)_{Mtc}$  represents the  $Mtc$  value obtained by the  $G_\Theta$  using all item features set  $\mathcal{F}$ , while  $G(\mathcal{F}_{\text{mask}}^i|\Theta)_{Mtc}$  represents the  $Mtc$  value obtained by the  $G_\Theta$  using features set which is set  $\mathcal{F}$  removing  $f_i$ . The same applies to  $G(\mathcal{F}_{\text{mask}}^{ij}|\Theta)_{Mtc}$ . It is worth noting that when  $E > 0$ , it indicates that the performance of the base model decreases after removing the feature, while  $E < 0$  indicates the performance of the base model improves. While  $E = 0$ , it means there is no influence on the performance of the base mode when removing corresponding feature(s).

## 4.2 Construction of $Q$ for QUBO

Since the QUBO problem is a minimization problem, we define  $Q$  as follows with counterfactual instances  $E$ :

$$Q_{ij} = \begin{cases} -E_i, & \text{if } i = j \\ -E_{ij}, & \text{if } i \neq j \end{cases} \quad (5)$$

Note that  $Q_{ii}$  considers only one feature  $f_i$ , while  $Q_{ij}$  considers the pair of features,  $f_i$  and  $f_j$ . This indicates that while the values of  $Q$  matter, how many features are considered to obtain those values also matter. Namely, the corresponding counterfactual instances in  $Q_{ij}$  when  $i \neq j$  would contain more information about features for feature selection purposes. This will be discussed and evaluated in the experiment Section 5.2.4.

After constructing  $Q$ , the feature selection will be solved as a QUBO problem to obtain the final selected features in  $\mathbf{x}$ , and the corresponding final selected feature set ( $\mathcal{F}^*$ ) will be used for the recommender systems.

## 4.3 Performance Analysis

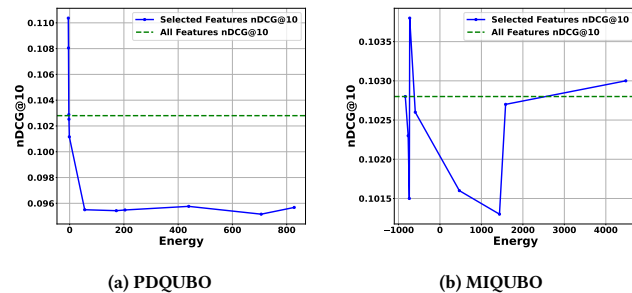


Figure 2: Energy Y vs nDCG@10

In this section, we attempt to answer why and how the proposed PDQUBO drives the optimization direction of the QUBO problem toward the optimization of recommendation performance. First, the aim of QUBO is to minimize the energy value  $Y$  as defined in Equation 1. So, it is reasonable to assume: that because PDQUBO is performance-driven, there must be a clear correlation between the

minimized  $Y$  values and the final recommendation performance when using the corresponding selected feature set. In order to investigate this, we conducted an analytic experiment: 50 features were randomly selected from the 150ICM dataset (detailed in Section 5), and PDQUBO and MIQUBO were deployed to select 45 features. The results are shown in Figure 2. It is observed that there is a clear and smooth negative correlation between  $Y$  and the final performance measured in nDCG@10 from PDQUBO, while there is an unclear trend in that of MIQUBO. This demonstrates that considering the relationship between features and the ground truth (e.g. Mutual Information) in MIQUBO cannot perform as well as considering the relationship between features and the recommendation performance in PDQUBO.

## 5 EXPERIMENT

### 5.1 Experimental Design

**5.1.1 Datasets:** We utilized two datasets, **150ICM** and **500ICM**, provided by CLEF 2024's QuantumCLEF Lab<sup>1</sup>, which focuses on benchmarking quantum annealing for information retrieval and recommender systems. The **150ICM** dataset comprises 1,881 users, 5,000 items, and 64,890 interactions, with 150 sparse features per item. The **500ICM** dataset contains 1,889 users, 7,000 items, and 68,062 interactions, featuring 500 sparse features per item. The sparsity of the features is 88.62% for 150ICM and 93.39% for 500ICM.

Followed by [18], an 80:20 split is applied to the data to construct the training and test sets. The training set is further divided using another 80:20 split, where 80% is used to train our PDQUBO model, and the remaining 20% is reserved for validation purposes. The final results are evaluated on the test set, with all reported metrics representing the average of 5 runs with random initialization.

**5.1.2 Baseline Models:** To benchmark the performance of our proposed PDQUBO model, we selected a set of well-established baseline models, including CQFS [43], MIQUBO, CoQUBO, and QUBO-Boosting [18]: • *i*) CQFS: Following [43], CQFS fills the coefficient matrix based on the item similarity from collaborative filtering and content-based models, but the collaborative filtering required for the method is the based model used in this paper. • *ii*) MIQUBO and CoQUBO: Following [18], MIQUBO fills the coefficient matrix with mutual information and conditional mutual information between features and labels, while CoQUBO fills the matrix with the correlation between features and labels. The classification labels are replaced with interactions in the recommender system, and interaction data undergoes 1:1 negative sampling. • *iii*) QUBO-Boosting: Following [18], QUBO-Boosting fills the coefficient matrix with the predicted values from the Support Vector Classifier and the true labels. The SVC is replaced with the base models.

**5.1.3 Metrics:** We evaluated model performance using the Normalized Discounted Cumulative Gain (nDCG), a metric that measures ranking quality by considering both the relevance of items and their positions within the top- $N$  recommendations. This is particularly effective for recommender systems, as it takes into account not only the presence of relevant items but also their order in the ranked list. We set  $N$  to 10 in this study.

<sup>1</sup>[https://clef2024.imag.fr/index.php?page=Pages/lab\\_pages/qclef.html](https://clef2024.imag.fr/index.php?page=Pages/lab_pages/qclef.html)

**5.1.4 Base Models:** To thoroughly evaluate the performance of the proposed PDQUBO model across various base recommendation models, we tested approaches ranging from classical methods to neural network-based models: • *i*) *Item-KNN* [50], a classical model that uses the user-item interaction matrix to predict potential interactions based on similarities calculated using item features; • *ii*) *MLP-DP/MLP-CON*, we developed two neural network-based models: MLP-DP and MLP-CON, both utilizing a Multi-Layer Perceptron (MLP [15]), to evaluate PDQUBO’s performance with different item feature processing strategies. These models allow us to investigate various methods for integrating item features. MLP-DP fuses the item’s latent embedding with its features, passing this combined data through an MLP. The result is then used in a dot product with the user’s embedding to predict interactions. MLP-CON, on the other hand, concatenates the item and user embeddings, along with the item’s features, into a single vector, which is passed through an MLP to generate predictions. Both models employ Bayesian Personalized Ranking (BPR [49]) loss with a 1:1 negative-to-positive sample ratio for optimization. These experiments provide valuable insights into how different feature processing techniques impact model prediction performance; • *iii*) *NCF* [29], Neural Collaborative Filtering (NCF) leverages both an MLP and Generalized Matrix Factorization (GMF) to model the non-linear and linear interactions between users and items. In this paper, we feed item features into an MLP to produce outputs matching the item embeddings’ dimensionality, which are then summed with the embeddings to integrate the features. This directly incorporates item features into the NCF architecture. Like MLP-DP and MLP-CON, we optimize NCF with BPR loss, maintaining a 1:1 ratio of negative to positive samples during training.

**5.1.5 Hyperparameter Tuning:** For Item-KNN, we utilized a fixed number of neighbors (we set it as 100 by following CLEF 2024’s QuantumCLEF Lab), to calculate predictions. For the neural network-based base models, a grid search [39] was performed to fine-tune key hyperparameters such as learning rate, batch size, and the number of layers. This optimization process was critical for achieving the best model performance and ensuring the accuracy of the counterfactual results.

**5.1.6 The Configuration of  $k$ :** The values of the number of features selected,  $k$  (in Equation 1) are set to [130, 135, 140, 145] for 150ICM, and [350, 400, 450, 470] for 500ICM. Additionally, we allow both PDQUBO and all baseline models to automatically determine the optimal number of features to maximize recommendation performance, indicated by \*.

**5.1.7 QUBO Optimization Methods:** To assess the performance of traditional versus quantum optimization techniques, we selected traditional methods that can be used to optimize QUBO problems, including Simulated Annealing (SA) [5], Stochastic Gradient Descent (SGD)[71], and Tabu Search (TS) [24] as comparison methods. These are compared against Quantum Annealing (QA) [47] and Hybrid [40] approaches implemented on D-Wave [40], both of which are Quantum Processing Unit (QPU). The Hybrid method, which integrates classical and quantum optimization, is particularly useful for addressing the limitations of quantum annealing when dealing with large-scale data that exceeds the available qubits [16]. The

comparison evaluates their optimization capabilities, computational efficiency, and scalability across different data sizes.

## 5.2 Experimental Results

**5.2.1 Baselines comparison:** This section provides a comprehensive analysis of PDQUBO’s performance compared to baseline models (CQFS, QUBO-Boosting, CoQUBO, and MIQUBO) across two datasets (150ICM and 500ICM), different optimization methods (SA, SGD, TS, QA, Hybrid), various number of features ( $k$ ), and base models (Item-KNN, MLP-DP, NCF, MLP-CON). Special attention is given to the case when  $k = *$ , where the model is allowed to automatically select the optimal number of features. We did not optimize models using the QA optimization method in the 500ICM dataset due to quantum computational limitations, with ‘-’ representing the cells where results are not available. All results of nDCG@10 are shown in Table 1.

In both 150ICM and 500ICM datasets, PDQUBO generally demonstrates strong performance across different optimization methods. However, there are scenarios where the baselines perform comparably or even better, depending on the optimization method, base models, and feature selection value. For the SA method, PDQUBO shows notable improvements in many cases. For example, in the Item-KNN model, when  $k = 130$ , the best-performing baseline is QUBO-Boosting with an nDCG@10 of 0.1021. PDQUBO achieves a higher score of 0.1140, reflecting an 11.7% improvement. Similarly, at  $k = 140$ , the best baseline is CQFS with 0.1015, while PDQUBO delivers 0.1121, marking a 10.4% gain. However, at  $k = 145$ , the gap narrows as PDQUBO achieves 0.1125, compared to QUBO-Boosting’s and CoQUBO’s 0.1028. While PDQUBO outperforms the baseline, the improvement is less pronounced at higher  $k$  values. In the case of SGD, PDQUBO shows mixed results. For example, in the MLP-DP, at  $k = 130$ , PDQUBO delivers 0.1331, compared to the best baseline CoQUBO with 0.1320, showing a modest 0.83% improvement. However, in the Item-KNN, NCF, and MLP-CON, the best-performing baselines nearly match PDQUBO, even better than PDQUBO at different values of  $k$ . For TS, PDQUBO also demonstrates competitive performance, particularly in the Item-KNN, and NCF at various  $k$ . For example, in the NCF, at  $k = 130$ , the best baseline is CQFS with an nDCG@10 of 0.1336, while PDQUBO achieves 0.1363, representing a 2.0% improvement. For QA, PDQUBO’s performance is also competitive in some cases. For instance, in the NCF, at  $k = *$ , PDQUBO achieves 0.1366, a slight improvement over the best baseline MIQUBO, which scores 0.1336. However, when  $k$  is set from 130 to 145, PDQUBO struggles to maintain competitive performance. For Hyrid, PDQUBO demonstrates particularly strong performance in Item-KNN, MLP-DP, and NCF. For example, in the NCF, at  $k = 145$ , PDQUBO achieves 0.1338, compared to CQFS’s 0.1331, representing a 0.53% improvement. Similar trends are observed in the 500ICM dataset, with the exception of the QA optimization method, which was not evaluated.

Across both datasets 150ICM and 500ICM, PDQUBO demonstrates superior performance over the baseline models in most of the cases. However, in some cases, the baselines perform comparably or even better, especially in SGD and QA optimization methods.

**5.2.2 Stability of QA:** We conducted experiments to examine the current stability of the used QA. As shown in Table 2, where letting

**Table 1: The performance of nDCG@10 using different optimization methods on various datasets under different base models. The bold text represents the best result of the five feature selection methods under the same conditions.**

Base Models			Item-KNN						MLP-DP						NCF						MLP-CON						
Models	Datasets	k	Traditional			QPU			Traditional			QPU			Traditional			QPU			Traditional			QPU			
			SA	SGD	TS	QA	Hybrid	SA	SGD	TS	QA	Hybrid	SA	SGD	TS	QA	Hybrid	SA	SGD	TS	QA	Hybrid	SA	SGD	TS	QA	Hybrid
CQFS	150ICM	*	0.0112	0.0095	0.0134	0.0495	0.0112	0.0108	0.0078	0.0176	0.0659	0.0108	0.0874	0.0868	0.0874	0.0868	0.0874	0.0042	0.0020	0.0047	0.0710	0.1062					
		130	0.0983	0.1029	0.0962	0.1009	0.0955	0.1328	0.1312	<b>0.1350</b>	0.1295	0.1343	0.1310	0.1308	0.1336	0.1304	0.1322	0.1102	0.1115	0.1144	0.1067	0.1163					
		135	0.0996	0.1035	0.0981	0.1008	0.1095	0.1320	0.1310	0.1342	0.1280	0.1321	0.1318	0.1306	0.1329	0.1251	0.1333	0.1133	0.1107	0.1123	0.0954	0.1149					
		140	0.1015	<b>0.1053</b>	0.1012	0.1051	0.1012	0.1330	0.1315	0.1331	0.1303	0.1331	0.1326	0.1318	0.1337	0.1315	0.1340	0.1167	0.1143	0.1154	0.1143	0.1167					
	500ICM	*	0.0034	0.0308	0.0275	-	0.0308	0.0001	0.0196	0.0209	-	0.0081	0.0706	0.1157	0.1157	-	0.1157	0.0033	0.0081	0.0088	-	0.0069					
		350	0.0103	0.1093	0.1067	-	0.1090	0.1397	0.1382	0.1220	-	0.1390	0.1219	0.1299	0.1183	-	0.1200	0.0942	0.1019	0.0842	-	0.0998					
		400	0.1074	<b>0.1096</b>	0.1056	-	0.1059	0.1408	0.1371	0.1331	-	0.1402	0.1274	0.1307	0.1201	-	0.1245	0.1037	0.1059	0.0932	-	0.0975					
		450	0.1120	<b>0.1102</b>	0.1163	-	0.1102	0.1406	0.1401	0.1429	-	0.1415	0.1295	0.1305	0.1269	-	0.1268	0.1085	0.1069	0.1065	-	0.1073					
QUBO-Boosting	150ICM	*	0.1028	0.1028	0.1028	0.1028	0.1028	0.1308	0.1308	0.1308	0.1308	0.1308	0.1336	0.1336	0.1336	0.1336	0.1336	0.1180	0.1180	0.1180	0.1180	0.1180					
		130	0.1021	0.1039	0.0954	0.0905	0.0952	0.1318	0.1314	0.1350	0.1288	0.1334	0.1301	0.1308	0.1305	0.1272	0.1305	0.1167	0.1089	0.1130	0.1142	0.1147					
		135	0.0968	0.1058	0.0969	0.0979	0.1012	0.1330	0.1306	<b>0.1360</b>	0.1311	0.1341	0.1310	0.1308	0.1296	0.1308	0.1324	0.1160	0.1118	0.1147	0.1129	0.1150					
		140	0.0986	0.1038	0.0987	0.0879	0.0967	0.1325	0.1304	<b>0.1350</b>	0.1335	0.1350	0.1316	0.1314	0.1324	0.1335	0.1324	0.1179	0.1131	0.1138	0.1168	0.1179					
	500ICM	*	0.1019	0.1027	0.1019	0.1056	0.1003	0.1323	0.1307	<b>0.1330</b>	0.1268	0.1323	0.1339	0.1320	0.1336	0.1264	0.1330	0.1180	0.1146	0.1166	0.1129	0.1178					
		350	0.1092	0.1092	0.1092	-	0.1092	0.1401	0.1401	0.1401	-	0.1401	0.1299	0.1299	0.1299	-	0.1299	0.1087	0.1087	0.1087	-	0.1087					
		400	0.0955	0.1144	0.0832	-	0.0897	0.1386	0.1375	0.1398	-	0.1371	0.1214	0.1291	0.1207	-	0.1174	0.0969	0.1052	0.0942	-	0.0938					
		450	0.0926	0.1093	0.0861	-	0.0937	0.1420	0.1381	<b>0.1413</b>	-	0.1403	0.1240	0.1298	0.1233	-	0.1240	0.0990	0.1078	0.0951	-	0.0996					
CoQUBO	150ICM	*	0.0319	0.0309	0.0323	0.0527	0.0319	0.0356	0.0253	0.0363	0.0486	0.0356	0.0293	0.0204	0.0347	0.0212	0.0293	0.0074	0.0057	0.0074	0.0094	0.0074					
		130	0.0948	<b>0.1033</b>	0.0941	0.0898	0.0946	0.1332	0.1320	0.1295	0.1332	0.1305	0.1263	0.1309	0.1259	0.1263	0.1244	0.1078	0.1105	0.0980	0.1102	0.1035					
		135	0.0973	0.1044	0.1009	0.0919	0.0983	0.1323	0.1308	0.1332	<b>0.1335</b>	0.1320	0.1280	0.1305	0.1284	0.1285	0.1280	0.1088	0.1079	0.1081	0.1100	0.1090					
		140	0.1007	0.1021	0.1028	0.1060	0.1028	0.1335	0.1309	0.1316	0.1333	0.1316	0.1307	0.1314	0.1322	0.1328	0.1322	0.1112	0.1128	0.1176	0.1137	0.1176					
	500ICM	*	0.0308	0.0436	0.0352	-	0.0309	0.0185	0.0278	0.0194	-	0.0180	0.0101	0.0113	0.0112	-	0.0092	0.0973	0.0151	0.0094	-	0.0078					
		350	0.0866	0.1153	0.0541	-	0.0693	0.1358	0.1387	0.1222	-	0.1157	0.1138	0.1295	0.0961	-	0.1030	0.0993	0.1115	0.0620	-	0.0736					
		400	0.0922	0.1079	0.0630	-	0.0749	0.1405	0.1397	0.1321	-	0.1371	0.1268	0.1314	0.1140	-	0.1139	0.0999	0.1084	0.0714	-	0.0846					
		450	0.1026	0.1076	0.0967	-	0.0923	0.1413	0.1407	0.1413	-	0.1412	0.1283	0.1320	0.1259	-	0.1264	0.1010	0.1090	0.0960	-	0.0948					
MIQUBO	150ICM	*	0.1028	0.1028	0.1028	0.1028	0.1028	0.1308	0.1308	0.1308	0.1308	0.1308	0.1336	0.1336	0.1336	0.1336	0.1336	0.1180	0.1180	0.1180	0.1180	0.1180					
		130	0.1018	<b>0.1040</b>	0.1022	0.1072	0.1033	0.1276	0.1307	0.1305	0.1335	0.1273	0.1314	0.1318	0.1315	0.1256	0.1300	0.1106	0.1138	0.1160	0.0938	0.1103					
		135	0.1021	0.1039	0.1018	0.0912	0.1020	0.1282	0.1300	0.1308	0.1255	0.1294	0.1315	0.1303	0.1320	0.1279	0.1323	0.1136	0.1069	<b>0.1181</b>	0.1099	0.1144					
		140	0.1028	0.1038	0.1032	0.1006	0.1027	0.1295	0.1305	0.1306	0.1307	0.1309	0.1320	0.1311	0.1333	0.1322	0.1324	0.1137	0.1119	0.1183	0.1137	0.1166					
	500ICM	*	0.1092	0.1092	0.1092	-	0.1092	0.1401	0.1401	0.1401	-	0.1401	0.1299	0.1299	0.1299	-	0.1299	0.1087	0.1087	0.1087	-	0.1087					
		350	0.1036	0.1101	0.1033	-	0.1069	0.1380	0.1374	0.1373	-	0.1355	0.1255	0.1316	0.1287	-	0.1251	0.0962	0.1036	<b>0.1098</b>	-	0.1022					
		400	0.1077	0.1093	0.1052	-	0.1150	0.1384	0.1394	0.1373	-	0.1368	0.1286	0.1315	<b>0.1306</b>	-	0.1259	0.1067	0.1098	<b>0.1106</b>	-	0.1074					
		450	0.1097	0.1089	0.1087	-	0.1086	0.1395	0.1399	0.1392	-	0.1377	0.1324	0.1301	0.1302	-	0.1279	<b>0.1118</b>	0.1088	0.1091	-	0.1044					
PDQUBO	150ICM	*	0.1168	<b>0.1168</b>	0.1168	<b>0.1168</b>	0.1168	0.1299	0.1299	0.1299	0.1299	0.1299	<b>0.1366</b>	<b>0.1366</b>	<b>0.1366</b>	<b>0.1366</b>	<b>0.1366</b>	0.1116	0.1116	0.1116	0.1116	0.1116					
		130	<b>0.1140</b>	0.1025	<b>0.1168</b>	0.0877	<b>0.1151</b>	<b>0.1366</b>	<b>0.1331</b>	0.1308	<b>0.1354</b>	<b>0.1346</b>	<b>0.1343</b>	0.1307	<b>0.1363</b>	0.1307	<b>0.1347</b>	0.1156	0.1106	0.1153	0.1117	0.1132					
		135	<b>0.1156</b>	0.1044	<b>0.1173</b>	0.0947	<b>0.1137</b>	<b>0.1350</b>	<b>0.1319</b>	0.1335	0.1299	<b>0.1350</b>	<b>0.1345</b>	0.1307	<b>0.1365</b>	0.1322	<b>0.1345</b>	0.1147	0.1089	0.1131	<b>0.1188</b>	0.1158					
		140	<b>0.1121</b>	0.1028	<b>0.1191</b>	0.1054	<b>0.1135</b>	<b>0.1356</b>	<b>0.1318</b>	0.1350	0.1293	<b>0.1355</b>	<b>0.1339</b>	0.1318	<b>0.1363</b>	0.1319	<b>0.1350</b>	0.1178	0.1156	<b>0.1193</b>	0.1140	<b>0.1193</b>					
	500ICM	*	0.1125	0.1029	<b>0.1116</b>	<b>0.1101</b>	<b>0.1116</b>	<b>0.1344</b>	<b>0.1316</b>	0.1322	0.1284	0.1322	<b>0.1345</b>	<b>0.1345</b>	0.1307	<b>0.1366</b>	<b>0.1366</b>	<b>0.1366&lt;/b</b>									

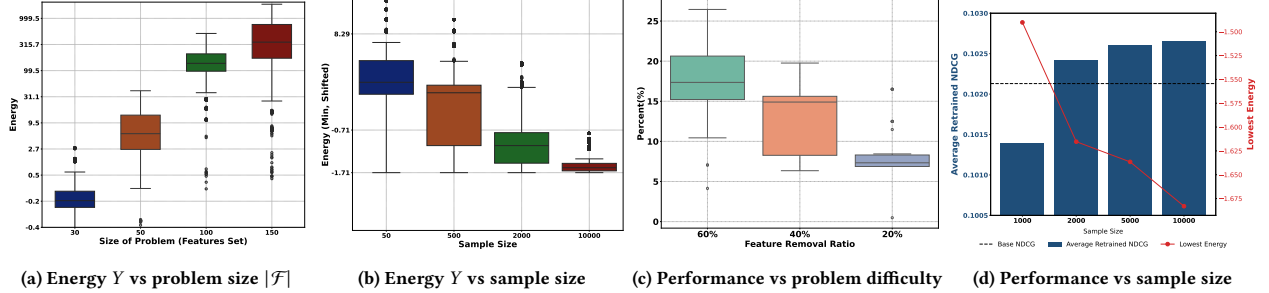


**Figure 3:** (a) Distribution of Energy values after selecting 90% of the features using QA. (b) This figure shows the lowest energy values achieved for a problem scale of 50, with 1000 repeated runs performed for each sample size. (c) Recommendation improvement vs the difficulty of the problem, which is defined as the percentage of feature values dropped from a fixed feature set. (d) Performance vs. sample size using varying numbers of QA samples. Each point shows the lowest energy and retrained model performance, averaged over 10 runs.

**Table 2: Comparison of energy Y with vs without constraints.** “without constraints” means optimizatin methods freely decide how many featrues to selection, while “with constrains” set  $k = 90\% \cdot |\mathcal{F}|$ .

scale $ \mathcal{F} $	without constraints			constraints ( $k = 90\% \cdot  \mathcal{F} $ )		
	SA	QA	Hybrid	SA	QA	Hybrid
10	-0.053	-0.052	-0.053	-0.051	-0.051	-0.051
30	-0.521	-0.521	-0.521	-0.511	-0.485	-0.511
50	-1.834	-1.834	-1.835	-1.758	2.3610	-1.767
100	-4.988	-4.988	-4.988	-4.621	18.494	-4.831
150	-8.908	-8.908	-8.908	-7.970	164.041	-8.206
300	-17.541	-	-17.541	-12.459	-	-13.331
500	-34.522	-	-34.523	-17.214	-	-20.255

that current QA methods remain stable only for small problem sizes but struggle to find optimal solutions as the problem size increases. • ii) the size of the samples: we examine the effect of varying QA sample sizes on optimization stability and downstream performance. As shown in Figure 3b and 3d, increasing the number of samples consistently reduces energy variance and helps the quantum annealer more reliably locate low-energy solutions. This improved stability leads to better feature subsets, which in turn enhance the recommendation model’s retrained performance. • iii) the difficulty of the problem: following [1], we use data sparsity to measure the difficulty of the problem. Specifically, we set the size of the feature set to 50, then we randomly drop the feature values from all features with certain percentage to get various feature sets with various sparsities. Specifically, we randomly drop 60%, 40% and 20% of feature values, then measure their corresponding relevant improvements to their corresponding recommendation performance with all feature performance (as shown in Figure 3c). It is observed that QA tends to get larger but less stable improvement when the problem is harder (the feature set is sparser).

**5.2.3 Efficiency of QUBO Optimization Methods:** To highlight the speed advantage of quantum annealers, we compared the solving times of QA, Hybrid, and classical methods (such as SA, SGD, and TS) across different problem scales in Table 3. The recorded times for QA and Hybrid only include the quantum sampling time on the QPU and the post-processing time for decoding annealing results. For QA, the number of samples was set to 2000, meaning that the annealing duration for a single QA process was less than 1e-4 seconds, making

**Table 3: Solving time vs. Problem scale.** Note that the QA line is shorter due to quantum computational limitations in D-wave [40].

Scale	Tradition			QPU	
	SA	SGD	TS	QA	Hybrid
10	1.85	0.102	1.62	0.202	8.73
30	2.26	0.832	2.17	0.178	9.6
50	5.03	2.15	4.21	0.443	8.85
100	13.65	8.55	12.51	0.496	9.51
150	29.36	18.67	26.3	0.546	9.68
300	138.93	75.48	133.58	-	13.32
500	391.03	212.19	472.01	-	16.49

the solving speed far superior to that of algorithms running on traditional computers. Furthermore, it can be observed that the solving times for the three classical methods increase exponentially with problem size, whereas the solving times for QA and Hybrid remain largely unaffected by problem scale.

**5.2.4 Necessity of Quadratic Terms:** We compare two counterfactual construction strategies for QUBO: removing two features simultaneously (“Comb”) versus removing a single feature (“Indiv”). Experiments on two base models (Item-KNN and MLP-DP) with datasets of size 150 and 500—where each result is averaged over five runs—show that when  $k = *$  (where the model is allowed to automatically select the optimal number of features), the “Comb” approach consistently outperforms “Indiv”, highlighting the advantage of modeling pairwise feature interactions. When  $k$  is fixed (as in table 1), “Indiv” occasionally performs better—approximately 1 out of 20 cases—but only when using the SA optimizer.

These rare cases motivated us to conduct 150 additional runs using the Hybrid method on the Item-KNN model at  $k = 135$  to validate whether the performance gap persists. The results show a mean nDCG@10 of 0.1151 for “Comb” and 0.1139 for “Indiv”. A Kolmogorov–Smirnov test (statistic = 0.2465,  $p = 7.84 \times 10^{-5}$ ) confirms that the performance difference is statistically significant. These findings reinforce the robustness of the “Comb” strategy and the importance of incorporating pairwise feature dependencies in QUBO-based feature selection.

**Table 4: Performance Comparison Between Quantum Algorithms and Traditional Feature Selection Algorithms in CTR Tasks**

Base Models	Methods	Avazu		Criteo		ICM_150		ICM_500	
		AUC	Logloss	AUC	Logloss	AUC	Logloss	AUC	Logloss
DeepFM	no_selection	0.74294	0.40105	0.76796	0.47816	0.84556	0.22260	0.84828	0.22176
	Lasso [53]	0.74252	0.40094	0.76764	0.47869	0.84510	0.22765	0.85228	0.22090
	GBDT [21]	0.74284	0.40095	0.76806	0.47844	0.84542	0.22303	0.84839	0.22168
	AutoField [62]	0.74318	0.40084	0.76831	0.47818	0.84510	0.22313	0.84806	0.22168
	LPFS [27]	0.74267	0.40099	0.76814	0.47824	<b>0.84795</b>	<u>0.22255</u>	<b>0.85473</b>	<u>0.22058</u>
	SFS [61]	0.74296	0.40082	0.76852	0.47789	0.84618	0.22278	0.85212	0.22247
	Permutation [20]	<b>0.74355</b>	<u>0.40057</u>	<u>0.76855</u>	0.47816	0.84640	0.22263	0.84874	0.22160
	SHARK [66]	0.74318	0.40060	0.76826	<u>0.47791</u>	0.84542	0.22306	0.85031	0.22131
	CQFS	0.74294	0.40105	0.76615	0.47946	0.84565	0.22285	0.85366	0.22056
	MIQUBO	0.74318	0.40084	0.76632	0.47954	0.84741	0.22272	0.85351	0.22049
	QUBO-Boosting	0.74266	0.40093	0.76770	0.47892	0.84201	0.22403	0.84657	0.22193
FiBiNET	CoQUBO	0.74254	0.40093	0.76703	0.47888	0.84405	0.22364	0.84694	0.22446
	PDQUBO_Indiv	0.74318	0.40060	0.76824	0.47799	0.84696	0.22276	0.85353	0.22062
	PDQUBO_SA	<u>0.74333</u>	<b>0.40048</b>	0.76820	0.47824	0.84695	0.22278	0.85317	0.22063
	PDQUBO_hybrid	<u>0.74333</u>	<b>0.40048</b>	<b>0.76857</b>	<b>0.47770</b>	0.84788	<b>0.22240</b>	<b>0.85456</b>	<b>0.22039</b>
	no_selection	0.74169	0.40148	0.77003	0.47697	0.83319	0.22802	0.83731	0.22558
	Lasso [53]	0.74114	0.40183	0.76972	0.47730	0.84241	0.22588	0.84503	0.22392
	GBDT [21]	0.74161	0.40157	0.77134	0.47605	0.84029	0.22631	0.84659	0.22334
	AutoField [62]	0.74161	0.40157	0.77141	0.47591	0.84150	0.22614	0.84584	0.22321
	LPFS [27]	0.74159	0.40158	0.77146	0.47584	<u>0.85546</u>	<b>0.22172</b>	<b>0.84883</b>	<b>0.22268</b>
	SFS [61]	0.74161	0.40157	0.77099	0.47621	0.85295	0.22271	0.84456	0.22336
	Permutation [20]	<u>0.74209</u>	<u>0.40138</u>	<u>0.77186</u>	0.47598	0.84050	0.22636	0.84220	0.22454
	SHARK [66]	0.74193	0.40146	0.77099	0.47621	0.83937	0.22670	0.84542	0.22369
	CQFS	0.74185	0.40154	0.77055	0.47646	0.83569	0.22771	0.22056	0.22471
	MIQUBO	0.74193	0.40146	0.77021	0.47698	0.84825	0.22414	0.84364	0.22444
	QUBO-Boosting	0.74191	0.40166	0.76906	0.47788	0.83569	0.22771	0.84306	0.22445
	CoQUBO	0.74169	0.40148	0.77060	0.47669	0.83886	0.22675	0.84028	0.22647
	PDQUBO_Indiv	0.74217	0.40131	0.77060	0.47669	0.85329	0.22255	0.84744	0.22317
	PDQUBO_SA	<b>0.74217</b>	<b>0.40131</b>	0.77157	<u>0.47583</u>	0.85511	0.22206	0.84771	0.22318
	PDQUBO_hybrid	0.74217	<u>0.40131</u>	<u>0.77197</u>	0.47561	<u>0.85567</u>	<u>0.22182</u>	<u>0.84864</u>	<u>0.22269</u>

### 5.3 PDQUBO vs Traditional Feature Selection

Here, we examine the performance differences between Quantum-based QUBO algorithms (including PDQUBO) and traditional feature selection methods implemented on classical computers. Although current quantum hardware still faces significant limitations in solving real-world problems, making such comparisons less than completely fair, it is still worth exploring. Considering that feature selection tasks in recommender systems are primarily applied to CTR scenarios, we incorporated two widely used CTR datasets, Avazu and Criteo, and applied a 1:5 negative sampling strategy to the ICM dataset to better align it with CTR tasks. Additionally, we replaced the base models with DeepFM [26] and FiBiNET [31], both implemented using the DeepCTR framework, and changed the evaluation metric from nDCG to AUC (Area under the curve) to better suit the CTR context. The dataset partitioning follows the approach outlined in Sec. 5.1. For traditional feature selection methods, we employed the benchmark proposed in ERASE [33] with default parameters to generate feature rankings. For QUBO algorithms on quantum architectures, to reduce the randomness inherent in solving quadratic problems, we repeated the selection process five times and adopted the feature selection results corresponding to the smallest  $Y$  value. Subsequently, the selected features were used to retrain the base models, instead of reusing the pre-trained model parameters as in previous experiments. To be fair, all hyperparameters of the retrained base models were kept consistent, including a fixed batch size of 1024 and an L2 regularization coefficient of 1e-5.

In Table 4, it is observed that PDQUBO\_hybrid consistently achieves the best or second-best performance across all scenarios (Note, according to the benchmark in feature selection [33, 66], even relatively small performance gains are considered meaningful). This demonstrates that, empowered by the precise and efficient optimization capabilities of quantum annealers, PDQUBO\_hybrid not only matches or surpasses traditional feature selection methods in performance but also exhibits greater stability across diverse datasets and models. In particular, PDQUBO significantly outperforms all QUBO-based baseline methods, confirming the effectiveness of the proposed performance-driven construction of the Q matrix. Compared to sensitivity-based methods such as Permutation, PDQUBO achieves substantial performance gains, especially on feature-rich datasets like ICM, where Permutation struggles. This improvement can be attributed to PDQUBO's ability to capture pairwise feature interactions during the selection process, as encoded in the quadratic terms of the QUBO matrix. Moreover, PDQUBO\_hybrid consistently outperforms or matches PDQUBO\_SA, highlighting the value of quantum annealers in more effectively exploring high-quality feature subsets. Notably, although the counterfactual instances  $E_i$  and  $E_{ij}$  in Equation 4 are derived during inference using pre-trained base models, the final recommendation models are re-trained with the selected features, ensuring generalizability of the selected subsets. The variant PDQUBO\_Indiv, which only uses diagonal elements in the Q matrix and ignores pairwise feature effects,

results in degraded performance. This further underscores the importance of incorporating interaction terms when constructing the QUBO formulation for feature selection. Finally, prior work such as ERASE [33] has shown that no single feature selection method consistently outperforms all others across every scenario. In contrast, PDQUBO\_hybrid demonstrates robust and competitive performance compared to both quantum and classical baselines, further validating its practical utility in recommender systems.

## 6 CONCLUSION

This paper proposed PDQUBO, a performance-driven QUBO method for recommender systems on quantum anneals, and it outperforms the state-of-the-art baselines models in terms of recommendation performance. Furthermore, based on the PDQUBO, we examined the stability of QA on the performance of recommendation problems and the necessity of the quadratic term in a QUBO-based recommender systems.

## References

- [1] G. Adomavicius and A. Tuzhilin. 2005. Toward the next generation of recommender systems: a survey of the state-of-the-art and possible extensions. *IEEE Transactions on Knowledge and Data Engineering* 17, 6 (2005), 734–749. <https://doi.org/10.1109/TKDE.2005.99>
- [2] Akshay Ajagekar and Fengqi You. 2023. Molecular design with automated quantum computing-based deep learning and optimization. *Npj Computational Materials* 9, 1 (2023), 143.
- [3] Tameem Albash and Daniel A Lidar. 2018. Demonstration of a scaling advantage for a quantum annealer over simulated annealing. *Physical Review X* 8, 3 (2018), 031016.
- [4] Alexandre Belloni, Tengyuan Liang, Hariharan Narayanan, and Alexander Raklin. 2015. Escaping the Local Minima via Simulated Annealing: Optimization of Approximately Convex Functions. *CoRR* abs/1501.07242 (2015). arXiv:1501.07242 <http://arxiv.org/abs/1501.07242>
- [5] Dimitris Bertsimas and John Tsitsiklis. 1993. Simulated annealing. *Statistical science* 8, 1 (1993), 10–15.
- [6] Munish Bhatia and Sandeep K Sood. 2020. Quantum computing-inspired network optimization for IoT applications. *IEEE Internet of Things Journal* 7, 6 (2020), 5590–5598.
- [7] Sergiu Boixo, Vadim N Smelyanskiy, Alireza Shabani, Sergei V Isakov, Mark Dykman, Vasil S Denchev, Mohammad H Amin, Anatoly Yu Smirnov, Masoud Mohseni, and Hartmut Neven. 2016. Computational multiqubit tunnelling in programmable quantum annealers. *Nature communications* 7, 1 (2016), 10327.
- [8] Avinash Chalamuk, Raghavendra Kune, and BS Manoj. 2021. A hybrid classical-quantum approach for multi-class classification. *Quantum Information Processing* 20, 3 (2021), 119.
- [9] Wei Chen, Yiqing Wu, Zhao Zhang, Fuzhen Zhuang, Zhongshi He, Ruobing Xie, and Feng Xia. 2024. FairGap: Fairness-aware recommendation via generating counterfactual graph. *ACM Transactions on Information Systems* 42, 4 (2024), 1–25.
- [10] Xu Chen, Yongfeng Zhang, and Ji-Rong Wen. 2022. Measuring "why" in recommender systems: A comprehensive survey on the evaluation of explainable recommendation. *arXiv preprint arXiv:2202.06466* (2022).
- [11] Yulin Chi, Jieshan Huang, Zhanchuan Zhang, Jun Mao, Zinan Zhou, Xiaojiong Chen, Chonghao Zhai, Jueming Bao, Tianxiang Dai, Huihong Yuan, et al. 2022. A programmable qudit-based quantum processor. *Nature communications* 13, 1 (2022), 1166.
- [12] Iris Cong, Soonwon Choi, and Mikhail D Lukin. 2019. Quantum convolutional neural networks. *Nature Physics* 15, 12 (2019), 1273–1278.
- [13] Washington Cunha, Celso França, Guilherme Fonseca, Leonardo Rocha, and Marcos André Gonçalves. 2023. An effective, efficient, and scalable confidence-based instance selection framework for transformer-based text classification. In *Proceedings of the 46th International ACM SIGIR Conference on Research and Development in Information Retrieval*. 665–674.
- [14] Prasanna Date, Davis Arthur, and Lauren Pusey-Nazzaro. 2021. QUBO formulations for training machine learning models. *Scientific reports* 11, 1 (2021), 10029.
- [15] Aminu Da'u and Naomie Salim. 2020. Recommendation system based on deep learning methods: a systematic review and new directions. *Artificial Intelligence Review* 53, 4 (2020), 2709–2748.
- [16] Michel H Devoret, Andreas Wallraff, and John M Martinis. 2004. Superconducting qubits: A short review. *arXiv preprint cond-mat/0411174* (2004).
- [17] Guglielmo Fagioli, Nicola Ferro, Raffaele Perego, and Nicola Tonello. 2024. Dimension importance estimation for dense information retrieval. In *Proceedings of the 47th International ACM SIGIR Conference on Research and Development in Information Retrieval*. 1318–1328.
- [18] Maurizio Ferrari Dacrema, Fabio Moroni, Riccardo Nembrini, Nicola Ferro, Guglielmo Fagioli, and Paolo Cremonesi. 2022. Towards feature selection for ranking and classification exploiting quantum annealers. In *Proceedings of the 45th International ACM SIGIR Conference on Research and Development in Information Retrieval*. 2814–2824.
- [19] Artur J Ferreira and Mário AT Figueiredo. 2012. Efficient feature selection filters for high-dimensional data. *Pattern recognition letters* 33, 13 (2012), 1794–1804.
- [20] Aaron Fisher, Cynthia Rudin, and Francesca Dominici. 2019. All models are wrong, but many are useful: Learning a variable's importance by studying an entire class of prediction models simultaneously. *Journal of Machine Learning Research* 20, 177 (2019), 1–81.
- [21] Jerome H Friedman. 2001. Greedy function approximation: a gradient boosting machine. *Annals of statistics* (2001), 1189–1232.
- [22] Yingqiang Ge, Shuchang Liu, Zuohui Fu, Juntao Tan, Zelong Li, Shuyuan Xu, Yunqi Li, Yikun Xian, and Yongfeng Zhang. 2022. A survey on trustworthy recommender systems. *ACM Transactions on Recommender Systems* (2022).
- [23] Fatih Gedikli, Dietmar Jannach, and Mouzhi Ge. 2014. How should I explain? A comparison of different explanation types for recommender systems. *International Journal of Human-Computer Studies* 72, 4 (2014), 367–382.
- [24] Fred Glover. 1990. Tabu search: A tutorial. *Interfaces* 20, 4 (1990), 74–94.
- [25] Fred Glover, Gary Kochenberger, and Yu Du. 2018. A tutorial on formulating and using QUBO models. *arXiv preprint arXiv:1811.11538* (2018).
- [26] Huifang Guo, Ruiming Tang, Yunning Ye, Zhenguo Li, and Xiuqiang He. 2017. DeepFM: a factorization-machine based neural network for CTR prediction. *arXiv preprint arXiv:1703.04247* (2017).
- [27] Yi Guo, Zhaocheng Liu, Jianchao Tan, Chao Liao, Sen Yang, Lei Yuan, Dongying Kong, Zhi Chen, and Ji Liu. 2022. LPFS: Learnable Polarizing Feature Selection for Click-Through Rate Prediction. *arXiv preprint arXiv:2206.00267* (2022).
- [28] Xiangnan He, Kuan Deng, Xiang Wang, Yan Li, Yongdong Zhang, and Meng Wang. 2020. LightGCN: Simplifying and powering graph convolution network for recommendation. In *Proceedings of the 43rd International ACM SIGIR conference on research and development in Information Retrieval*. 639–648.
- [29] Xiangnan He, Lizi Liao, Hanwang Zhang, Liqiang Nie, Xia Hu, and Tat-Seng Chua. 2017. Neural collaborative filtering. In *Proceedings of the 26th international conference on world wide web*. 173–182.
- [30] Jonathan L Herlocker, Joseph A Konstan, Loren G Terveen, and John T Riedl. 2004. Evaluating collaborative filtering recommender systems. *ACM Transactions on Information Systems (TOIS)* 22, 1 (2004), 5–53.
- [31] Tongwen Huang, Zhiqi Zhang, and Junlin Zhang. 2019. FiBiNET: combining feature importance and bilinear feature interaction for click-through rate prediction. In *Proceedings of the 13th ACM conference on recommender systems*. 169–177.
- [32] Kalervo Järvelin and Jaana Kekäläinen. 2002. Cumulated gain-based evaluation of IR techniques. *ACM Transactions on Information Systems (TOIS)* 20, 4 (2002), 422–446.
- [33] Pengyu Jia, Yeqing Wang, Zhaocheng Du, Xiangyu Zhao, Yichao Wang, Bo Chen, Wanyu Wang, Huifang Guo, and Ruiming Tang. 2024. Erase: Benchmarking feature selection methods for deep recommender systems. In *Proceedings of the 30th ACM SIGKDD Conference on Knowledge Discovery and Data Mining*. 5194–5205.
- [34] Tadashi Kadowaki and Hidetoshi Nishimori. 1998. Quantum annealing in the transverse Ising model. *Phys. Rev. E* 58 (Nov 1998), 5355–5363. Issue 5. <https://doi.org/10.1103/PhysRevE.58.5355>
- [35] Thaddeus D Ladd, Fedor Jelezko, Raymond Laflamme, Yasunobu Nakamura, Christopher Monroe, and Jeremy Lloyd O'Brien. 2010. Quantum computers. *nature* 464, 7285 (2010), 45–53.
- [36] Weilin Lin, Xiangyu Zhao, Yeqing Wang, Tong Xu, and Xian Wu. 2022. AdaFS: Adaptive feature selection in deep recommender system. In *Proceedings of the 28th ACM SIGKDD Conference on Knowledge Discovery and Data Mining*. 3309–3317.
- [37] Yaxu Liu, Jui-Nan Yen, Bowen Yuan, Rundong Shi, Peng Yan, and Chih-Jen Lin. 2022. Practical counterfactual policy learning for top-k recommendations. In *Proceedings of the 28th ACM SIGKDD Conference on Knowledge Discovery and Data Mining*. 1141–1151.
- [38] Seth Lloyd, Masoud Mohseni, and Patrick Rebentrost. 2014. Quantum principal component analysis. *Nature physics* 10, 9 (2014), 631–633.
- [39] Rafael G Mantovani, André LD Rossi, Joaquim Vanschoren, Bernd Bischl, and André CPLF De Carvalho. 2015. Effectiveness of random search in SVM hyperparameter tuning. In *2015 international joint conference on neural networks (IJCNN)*. Ieee, 1–8.
- [40] Catherine C. McGeoch and Pau Farré. 2020. The D-Wave Advantage System: An Overview TECHNICAL REPORT. <https://api.semanticscholar.org/CorpusID:22235574>
- [41] Satoshi Morita and Hidetoshi Nishimori. 2008. Mathematical foundation of quantum annealing. *J. Math. Phys.* 49, 12 (2008).
- [42] Sascha Mücke, Raoul Heese, Sabine Müller, Moritz Wolter, and Nico Piatkowski. 2023. Feature selection on quantum computers. *Quantum Machine Intelligence* 5, 1 (2023), 11.
- [43] Riccardo Nembrini, Maurizio Ferrari Dacrema, and Paolo Cremonesi. 2021. Feature selection for recommender systems with quantum computing. *Entropy* 23, 8 (2021), 970.
- [44] Andrea Pasin, Washington Cunha, Marcos André Gonçalves, and Nicola Ferro. 2024. A quantum annealing instance selection approach for efficient and effective transformer fine-tuning. In *Proceedings of the 2024 ACM SIGIR International Conference on Theory of Information Retrieval*. 205–214.
- [45] Davide Pastorello and Enrico Blanzieri. 2019. Quantum annealing learning search for solving QUBO problems. *Quantum Information Processing* 18, 10 (2019), 303.
- [46] Hanchuan Peng, Fuhui Long, and Chris Ding. 2005. Feature selection based on mutual information criteria of max-dependency, max-relevance, and min-redundancy. *IEEE Transactions on pattern analysis and machine intelligence* 27, 8 (2005), 1226–1238.
- [47] Atanu Rajak, Sei Suzuki, Amit Dutta, and Bikas K Chakrabarti. 2023. Quantum annealing: An overview. *Philosophical Transactions of the Royal Society A* 381, 2241 (2023), 20210417.
- [48] Patrick Rebentrost, Masoud Mohseni, and Seth Lloyd. 2014. Quantum support vector machine for big data classification. *Physical review letters* 113, 13 (2014), 130503.
- [49] Steffen Rendle, Christoph Freudenthaler, Zeno Gantner, and Lars Schmidt-Thieme. 2012. BPR: Bayesian personalized ranking from implicit feedback. *arXiv preprint arXiv:1205.2618* (2012).

[50] Badrul Sarwar, George Karypis, Joseph Konstan, and John Riedl. 2001. Item-based collaborative filtering recommendation algorithms. In *Proceedings of the 10th international conference on World Wide Web*. 285–295.

[51] Juntao Tan, Shijie Geng, Zuohui Fu, Yingqiang Ge, Shuyuan Xu, Yunqi Li, and Yongfeng Zhang. 2022. Learning and evaluating graph neural network explanations based on counterfactual and factual reasoning. In *Proceedings of the ACM web conference 2022*. 1018–1027.

[52] Juntao Tan, Shuyuan Xu, Yingqiang Ge, Yunqi Li, Xu Chen, and Yongfeng Zhang. 2021. Counterfactual explainable recommendation. In *Proceedings of the 30th ACM International Conference on Information & Knowledge Management*. 1784–1793.

[53] Robert Tibshirani. 1996. Regression shrinkage and selection via the lasso. *Journal of the Royal Statistical Society Series B: Statistical Methodology* 58, 1 (1996), 267–288.

[54] Nava Tintarev and Judith Masthoff. 2015. Explaining recommendations: Design and evaluation. In *Recommender systems handbook*. Springer, 353–382.

[55] Kari Torkkola. 2003. Feature extraction by non-parametric mutual information maximization. *Journal of machine learning research* 3, Mar (2003), 1415–1438.

[56] Khanh Hiep Tran, Azin Ghazimatin, and Rishiraj Saha Roy. 2021. Counterfactual explanations for neural recommenders. In *Proceedings of the 44th International ACM SIGIR Conference on Research and Development in Information Retrieval*. 1627–1631.

[57] Sahil Verma, Varich Boonsanong, Minh Hoang, Keegan Hines, John Dickerson, and Chirag Shah. 2020. Counterfactual explanations and algorithmic recourses for machine learning: A review. *Comput. Surveys* (2020).

[58] Jianwei Wang, Stefano Paesani, Raffaele Santagati, Sebastian Knauer, Antonio A Gentile, Nathan Wiebe, Maurangelo Petruzzella, Jeremy L O'brien, John G Rarity, Anthony Laing, et al. 2017. Experimental quantum Hamiltonian learning. *Nature Physics* 13, 6 (2017), 551–555.

[59] Xiangmeng Wang, Qian Li, Dianer Yu, Qing Li, and Guandong Xu. 2024. Counterfactual explanation for fairness in recommendation. *ACM Transactions on Information Systems* 42, 4 (2024), 1–30.

[60] Xiangmeng Wang, Qian Li, Dianer Yu, Qing Li, and Guandong Xu. 2024. Reinforced path reasoning for counterfactual explainable recommendation. *IEEE Transactions on Knowledge and Data Engineering* (2024).

[61] Yeqing Wang, Zhaocheng Du, Xiangyu Zhao, Bo Chen, Huifeng Guo, Ruiming Tang, and Zhenhua Dong. 2023. Single-shot feature selection for multi-task recommendations. In *Proceedings of the 46th International ACM SIGIR Conference on Research and Development in Information Retrieval*. 341–351.

[62] Yeqing Wang, Xiangyu Zhao, Tong Xu, and Xian Wu. 2022. Autofield: Automating feature selection in deep recommender systems. In *Proceedings of the ACM Web Conference 2022*. 1977–1986.

[63] Zhenlei Wang, Jingsen Zhang, Hongteng Xu, Xu Chen, Yongfeng Zhang, Wayne Xin Zhao, and Ji-Rong Wen. 2021. Counterfactual data-augmented sequential recommendation. In *Proceedings of the 44th international ACM SIGIR conference on research and development in information retrieval*. 347–356.

[64] Sheir Yarkoni, Elena Raponi, Thomas Bäck, and Sebastian Schmitt. 2022. Quantum annealing for industry applications: Introduction and review. *Reports on Progress in Physics* 85, 10 (2022), 104001.

[65] Dianlong You, Shina Niu, Siqi Dong, Huigui Yan, Zhen Chen, Di Wu, Limin Shen, and Xindong Wu. 2023. Counterfactual explanation generation with minimal feature boundary. *Information Sciences* 625 (2023), 342–366.

[66] Beichuan Zhang, Chenggen Sun, Jianchao Tan, Xinjun Cai, Jun Zhao, Mengqi Miao, Kang Yin, Chengyu Song, Na Mou, and Yang Song. 2023. SHARK: A Lightweight Model Compression Approach for Large-scale Recommender Systems. In *Proceedings of the 32nd ACM International Conference on Information and Knowledge Management*. 4930–4937.

[67] Shengyu Zhang, Dong Yao, Zhou Zhao, Tat-Seng Chua, and Fei Wu. 2021. Causerec: Counterfactual user sequence synthesis for sequential recommendation. In *Proceedings of the 44th International ACM SIGIR Conference on Research and Development in Information Retrieval*. 367–377.

[68] Yongfeng Zhang, Guokun Lai, Min Zhang, Yi Zhang, Yiqun Liu, and Shaoping Ma. 2014. Explicit factor models for explainable recommendation based on phrase-level sentiment analysis. In *Proceedings of the 37th international ACM SIGIR conference on Research & development in information retrieval*. 83–92.

[69] Linghua Zhu, Ho Lun Tang, George S Barron, FA Calderon-Vargas, Nicholas J Mayhall, Edwin Barnes, and Sophia E Economou. 2022. Adaptive quantum approximate optimization algorithm for solving combinatorial problems on a quantum computer. *Physical Review Research* 4, 3 (2022), 033029.

[70] Yaochen Zhu, Jing Ma, Liang Wu, Qi Guo, Liangjie Hong, and Jundong Li. 2023. Path-specific counterfactual fairness for recommender systems. In *Proceedings of the 29th ACM SIGKDD Conference on Knowledge Discovery and Data Mining*. 3638–3649.

[71] Martin Zinkevich, Markus Weimer, Lihong Li, and Alex Smola. 2010. Parallelized stochastic gradient descent. *Advances in neural information processing systems* 23 (2010).